Moringa oleifera Phytochemical Composition and the Influence of Environmental Growing Conditions

Tanner R. Sciara, Jennifer Perry Cecile, Chishimba Nathan Mowa, Claudia P. Cartaya-Marin

Honors Thesis

Appalachian State University

Boone, NC 28608

Moringa oleifera Phytochemical Composition and the Influence of
Environmental Growing Conditions

by

Tanner R. Sciara

Honors Thesis

Appalachian State University

Submitted to the A. R. Smith Department of Chemistry
and The Honors College
in partial fulfillment of the requirements for the degree of

Bachelor of Science

May, 2018

Approved by:

_____
Jennifer Perry Cecile, Ph.D., Thesis Director

_____
Chishimba Nathan Mowa, Ph.D., Second Reader

_____
Claudia P. Cartaya-Marin, Ph.D., Chair, Third Reader

_____
Libby G. Puckett, Ph.D., Departmental Honors Director

_____
Jefford Vahlbusch, Ph.D., Dean, The Honors College

Acknowledgements

Funding and support for this project originated from the

Office of Student Research, and the A. R. Smith Department of Chemistry.

Research advisors included,

Dr. Jennifer Perry Cecile, and

Dr. Libby G. Puckett

Additional Faculty involved:

Dr. Chishimba Nathan Mowa, and

Dr. Claudia P. Cartaya-Marin

Student involved in aspects of this project:

Franchesca Uribe Rheinbolt

I would like to thank all the faculty and student listed above for their insight and assistance over the course of this project.

I would like to thank my Dad, Steve, my Mom, Nancy, and my sister, Aubrey for their words of wisdom and encouragement while I attended Appalachian State University. They are not only my family, but also the best friends I could ask for.

Abstract

Moringa oleifera is a useful plant in many aspects. It contains a large amount of necessary nutrients for humans including protein, vitamins, and minerals. It also could be used for other purposes such as biofuel, animal fodder, and as a water clarifier. In this work a *M. oleifera* ethanolic extract reconstituted in borate buffer was analyzed using absorbance, fluorescence, and capillary electrophoresis for the presumptive and quantitative measurement of the phytochemical isoquercetin. The absorbance and fluorescence data presumptively indicated that isoquercetin was present in the extract along with other phytochemicals in the phenol, terpenoid, and flavonoid phytochemical classes. Capillary electrophoresis electropherogram data with the neutral marker mesityl oxide indicated that the species of interest on the electropherogram were anionic, especially the peak analyzed for standard addition. A standard addition of isoquercetin using capillary electrophoresis separation resulted in a calculated extract concentration of 312 ± 42 µM isoquercetin. A repeat standard addition is necessary to increase precision of the isoquercetin concentration. Another aspect of this project was creating a UV supplemented, hydroponic growing model for *M. oleifera* in order to stimulate more phytochemical production. Prototype results were promising, however, the completed model grew plants with an abnormal morphology. Further testing is needed to determine the cause before plants grown with the model can be analyzed using the aforementioned techniques.

Table of Contents

List of Figures

List of Abbreviations

CE	Capillary Electrophoresis
CFL	Compact Fluorescent Light
EMS	Electro-magnetic Spectrum
EMR	Electro-magnetic Radiation
HPLC	High Performance Liquid Chromatography
LIF	Laser Induced Fluorescence
LED	Light Emitting Diode
MEKC	Micellular Electrokinetic Chromatography
MS	Mass Spectrometry
MS/MS	Tandem Mass Spectrometry
PAS	Photosystem Antenna Complex
Phe	Phenolic
UV	Ultra-violet
UVA	Ultra-violet A
UVB	Ultra-violet B
UVC	Ultra-violet C

Introduction: *Moringa oleifera*

<u>Botany</u>

      The *Moringa* genus is solitary under the Moringaceae family and consists of 13 species. Each of the species is found under three distinct clades known as the bottle tree, the tuberous, and the slender tree. *M. oleifera*, *M. concanensis* and *M. peregrina* originate from the Indian subcontinent and Arabian Peninsula. They are all grouped into the slender tree clade[1].

      M. oleifera (Figure 1) has spread to at least 70 countries and can grow in sub-tropical and tropical regions with preferential semi-arid or monsoon climates. Annual precipitation ranges for growth are between 250-3000 mm. The capability of the plant to withstand significant drought stress is due to a large underground rootstock and a deciduous nature when water is scarce[1]. *M. oleifera* can handle temperatures as high as 48°C and as low as 0°C for short periods of time. It is also tolerant of saline soils and can grow in clay, silt, and sandy soils with a pH range of 5-9[1].

      M. oleifera has the ability to grow 3-4 meters in one year and can also produce flowers two years after germination and 6-12 months after planting stem cuttings. Matured *M. oleifera* can have up to ten flowering cycles a year and roughly three quarters of these flowers are fertilized with cross pollination. Mature plants can also produce a maximum of 20,000 seeds a year with an immediate 80% germination rate[1].

Figure 1. *M. oleifera* in Vieques, Puerto Rico.

M. oleifera has been used in history by Indians, Egyptians and Greeks, and Romans were aware of its uses. Despite this, research on *M. oleifera* only began in the 1990's and its health benefits were discovered while studying parts of the seed[2]. Multiple parts of the plant such as seeds, leaves, flowers, sap, bark, and roots have been utilized[3]. The leaves are the most commonly used structure of the plant and contain compounds with numerous health benefits (see section Phytochemicals). They are used for human nutrition and animal fodder as they have several vitamins and minerals and contain a protein content of roughly 30%[2,3]. Traditionally the leaves are used for malaria, typhoid fever, parasites, swelling, lesions, diabetes, and hypertension. The bark has usually been boiled in water or soaked in alcohol to make drinks for stomach ailments, joint pain, diabetes, toothaches, and anemia[2]. The roots have been soaked in water or alcohol to make remedies and the flowers also have their traditional uses. *M. oleifera* seeds have a flocculent property that functions using proteins to coagulate sediment and debris in water. Additionally, the seeds contain 30-40% oil that can be used for cooking or biodiesel as it has strong oxidative resistance[2]. Currently there are commercial *M. oleifera* operations in India, South and Central America, Africa, and Hawaii[3].

Ultra-violet and Photosynthetically Active Radiation

Ultraviolet radiation (UV) is composed of ultra-violet A (UVA 400-315 nm), ultra-violet B (UVB 315-280 nm), and ultra-violet C (UVC 280-100 nm). When going from UVA to UVC regions of the electromagnetic spectrum (EMS), wavelength decreases and photon energy increases. Atmospheric ozone functions as a partial UV shield as it absorbs nearly all of the high energy UVC or shortwave ultra-violet radiation and allows UVB and UVA to enter the atmosphere. Photosynthetically active radiation (PAR) is composed of wavelengths

in the 400-700 nm range which is also the visible range of the EMS. This means that under normal environmental conditions plants must deal with EMR exposure in the approximate 280-700 nm range. Infrared wavelengths may pose issues for plants in terms of heat regulation, but that was not a focal point of this research. Additionally, other atmospheric events such as cloud cover may affect EMR exposure. The atmospheric transmission of certain wavelengths can be seen in Figure 2. Nearly all visible and partial longer wave UV radiation is transmitted to the surface of the Earth.

Figure 2. Atmospheric transmission as a function of wavelength[4].
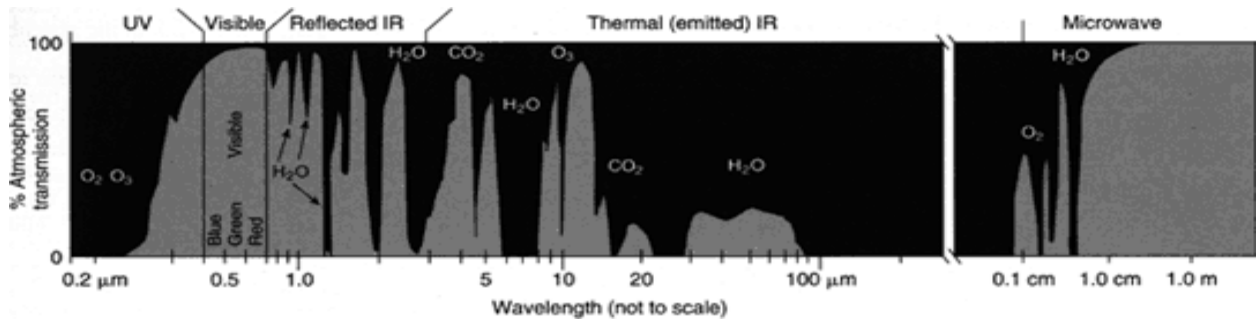
Under natural environmental conditions, plants are exposed to UVA radiation at 10-100 times the amount of UVB radiation. The hourly and seasonal change in UVA radiation is also less than UVB radiation[5]. Under UVB radiation exposure, heavy absorption occurs in the plant exterior and thus limited transmission reaches the interior regions of the plant. This type of radiation can cause direct damage to plant tissue[6]. UVA radiation can penetrate deeper into tissue and can cause secondary damage through reactive oxygen species[6].

Plants produce several different types of photo-protective pigments to reduce exposure to the aforementioned wavelengths as well as other environmental conditions[6]. In order for a pigment to be considered photo-protective, it generally needs to meet three criteria. Firstly, it must absorb wavelengths that are consistent with the absorption of the chemical components being protected. Secondly, cells must synthesize these pigments in

response to a spectral stimulus in the correct wavelength range. Thirdly, the production of the pigment must provide some resistance to the spectral stimulus[6]. These photo-protective pigments are documented to possess a high photo-stability. This allows plants to invest a large energy input into the pigment production, and minimal energy input into pigment maintenance over long term environmental stressors[6]. This is of particular use to plant epidermal cells which excrete phenolic acids and flavonols bound to long chain fatty acids. These chemicals make an effective barrier known as the cuticle[6]. Other plant components that are responsible for photo-protection include vacuoles, chloroplasts, plastoglobuli, and cytoplasmic lipid globules. Vacuoles of the epidermis can contain phenolic acids, flavonols, and anthocyanins. Chloroplasts use carotenoids near the photosystem antenna complex (PSA) to dissipate excess harvested energy. Plastoglobuli and cytoplasmic lipid globules both contain carotenoids[6]. A pictorial representation of these components in a cross-sectional view is shown in Figure 3. Further discussion on the photo-protective pigments/phytochemicals is available in the Phytochemicals section.
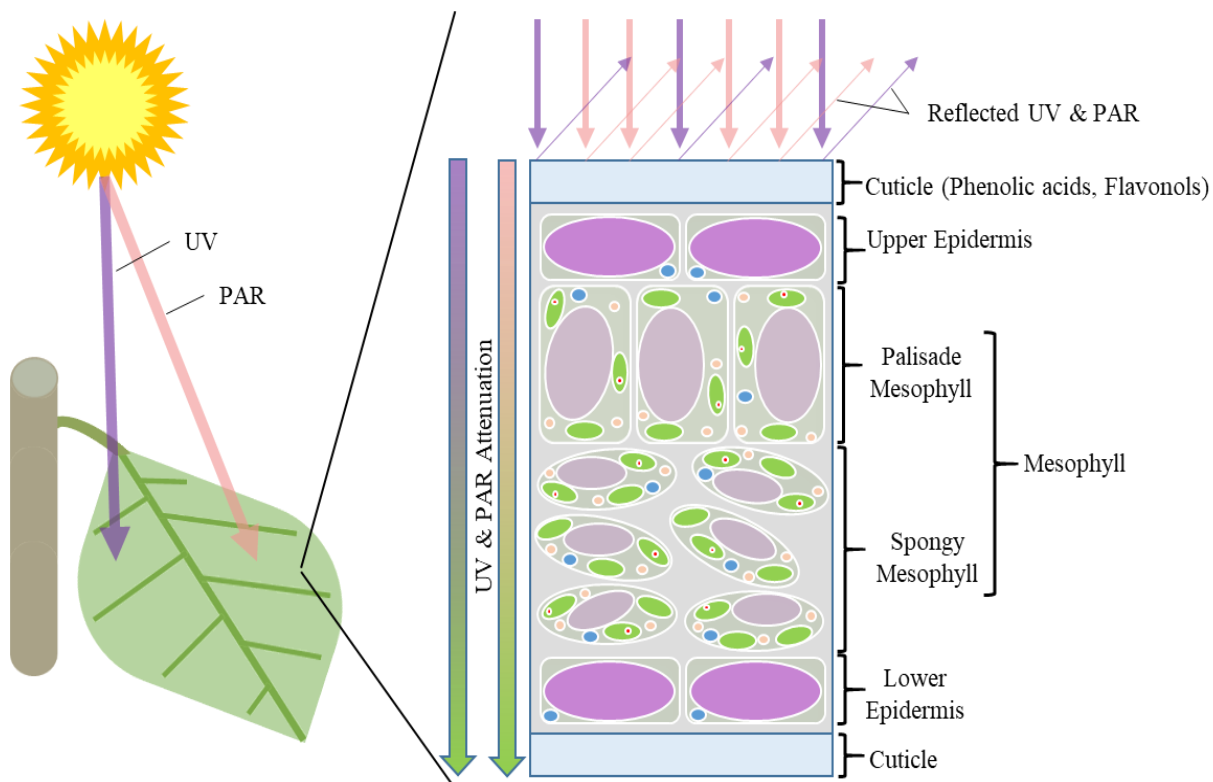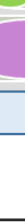
Diagram Part Name	Diagram Part	Protective Components
Vacuole		Phenolic acids, Flavonols, Anthocyanins
Chloroplast		Violaxanthin Cycle
Nucleus		N/A
Cell		N/A
Plastoglobuli		Carotenoids
Cytoplasmic Lipid Globules		Carotenoids and Fatty Acid Esters

Figure 3. Cross-sectional view of a plant leaf with the phytochemical components responsible for photo-protection. This figure was adapted from Figure 1 in reference 6.

Under greenhouse grown conditions, *M. oleifera* could produce different quantities of phytochemicals than when present in an outdoor environemnt. Many types of greenhouse covers and paneling are advertised to absorb UV wavelengths. The UV attenuation could adversely affect the quantity and quality of various phytochemcials of medical interest since

some of these function as photo-protective components of plants. A depiction of this is shown in Figure 4.
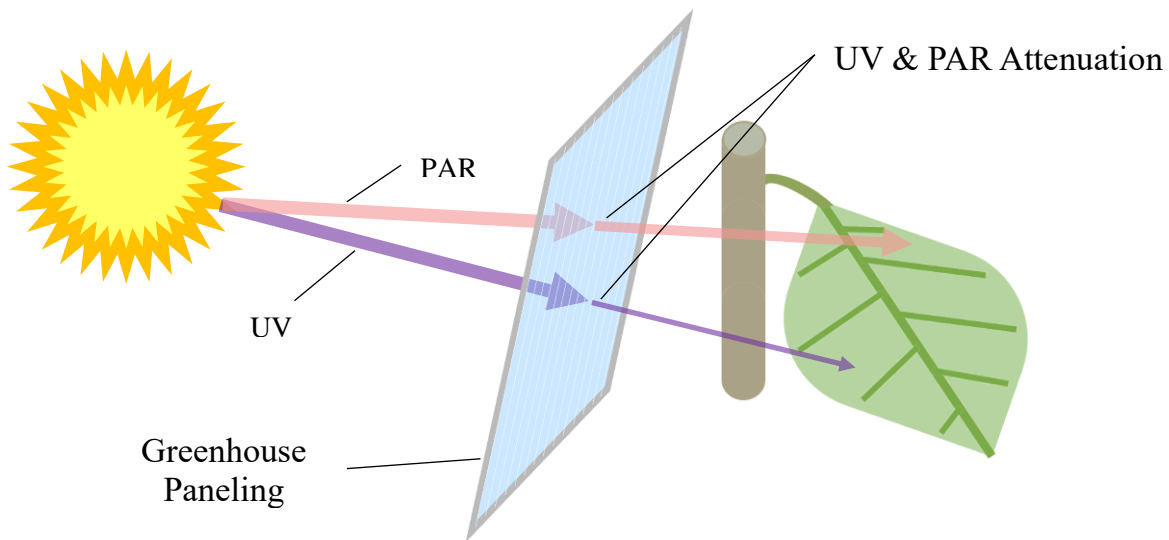
Figure 4. UV and PAR attenuation from greenhouse paneling.

Phytochemicals

The use of phenolic (Phe) compounds is ubiquitous in the plant kingdom and greater than 100,000 unique Phe compounds are known[6]. These compounds can be separated into phenolic acids, phenols, phenylpropanoids, flavonols, and anthocyanins and several sub-categories. They have structures that contain at least one aromatic ring with the presence of a hydroxyl group and other possible groups. In the case of phenolic acids, a carboxylic acid group is present and in the case of phenylpropanoids, a three carbon chain is present as displayed in Figure 5. These structures and the synthesis pathways of the Phe are used for naming individual chemical species[6]. Many Phe compounds are transported into the vacuole of plant cells and the cuticle of the leaf where they can serve as photo-protective components. This mechanism is the result of Phe UVB and UVA absorption with wavelength max points at roughly 280 and 300-360nm[6]. The former peak is the result of an aromatic ring structure

and is found in all Phe species. The latter peak is more variable and differs depending on the subcategory of the Phe compound. In the case of anthocyanins the second wavelength max point is located at roughly 525 nm[6].
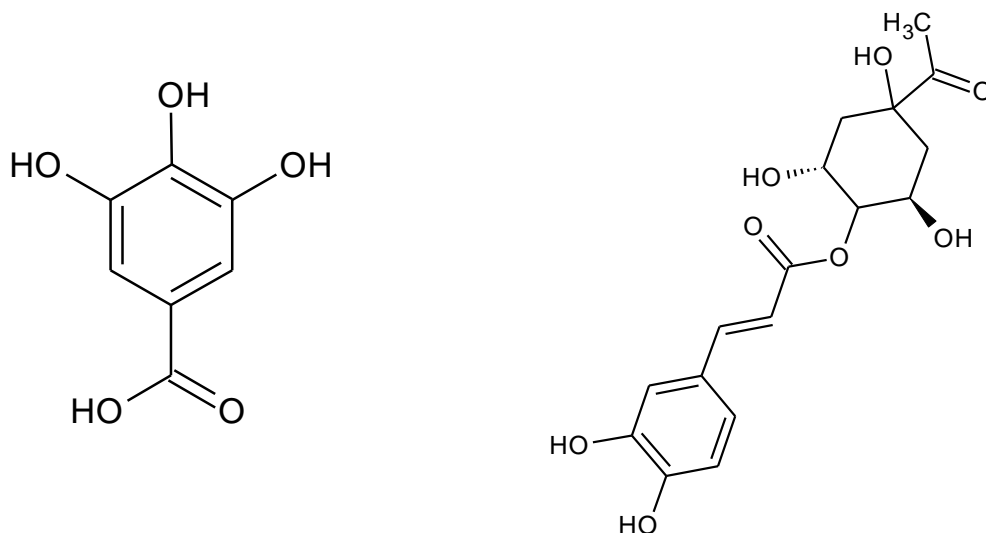
Figure 5. Chemical structures of two phenolic species found in *M. oleifera* (left to right): gallic acid (phenolic acid) and crypto-chlorogenic acid (phenylpropanoid).

Carotenoids are terpenoids and are also widely distributed among plants with greater than 800 known carotenoid compounds, some of which have linear and/or cyclic structures[6]. Carotenoids function as scavengers for free radicals and can quench chlorophyll triplets and singlet oxygen. They can also function in harvesting the excited state energy of chlorophyll and dissipating it thermally through the xanthophyll cycle in the thylakoid. This protects the PSA from light damage. The absorbance profiles of these compounds are dependent on the quantity of conjugated bonds, and the quantity and quality of substituents on the carbon chain[6](example structure displayed in Figure 6). Some of the more important and well known carotenoids have absorbance maxima that range from 400-500 nm and typically appear with two minor peaks[7].
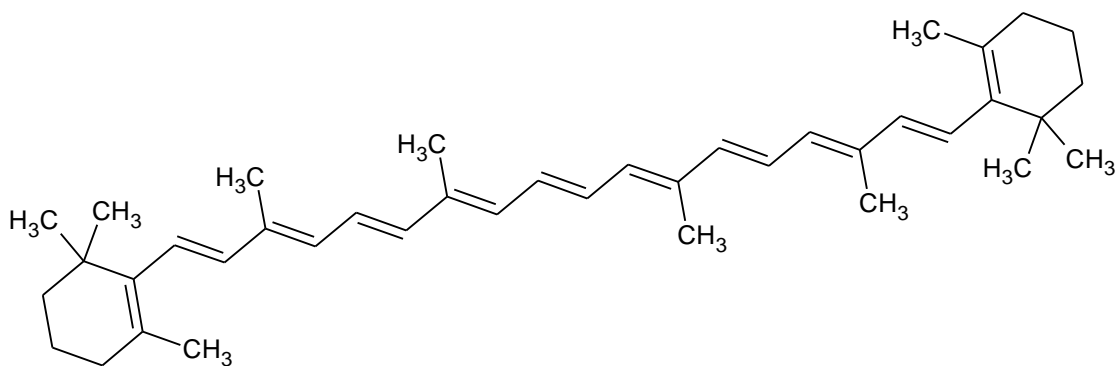
Figure 6. Chemical structure of the terpenoid beta-carotene, which can be found in *M. oleifera*.

There are numerous phytochemical components in *M. oleifera*. These are collectively shown in Figure 7, but the figure is likely not exhaustive. The phytochemicals are grouped into phytochemical classes as well as the biological properties of the phytochemicals.
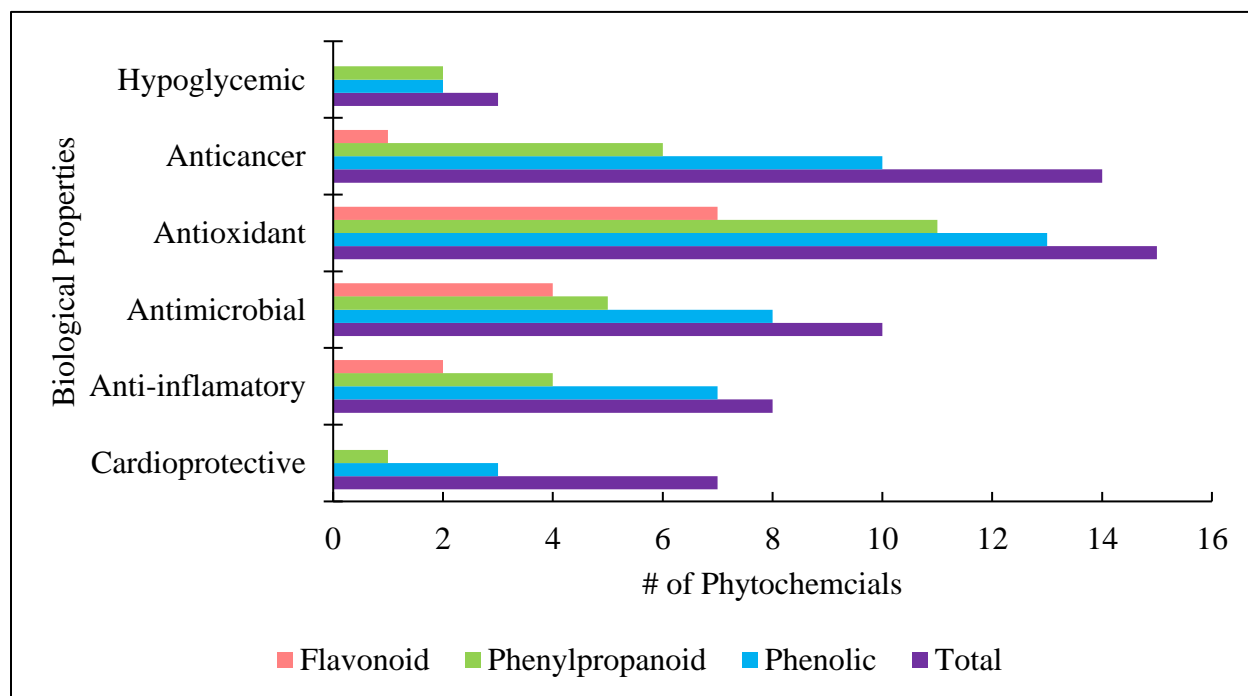
Figure 7. Phytochemical components found in *M. oleifera* and their biological properties[2,3,8]. Information for this chart was collected and processed by Franchesca Uribe Rheinbolt.

Isoquercetin

Isoquercetin is an important component of this research and has been quantitated before in *M. oleifera*[9]. Isoquercetin is a flavanol composed of quercetin and a beta-glucoside. It is one of the well-known flavanols and has functionality as an anti-oxidant,

anti-inflammatory, and anti-allergic phytochemical. It also has better bioavailability compared to its aglycone relative quercetin[10]. The structure of isoquercetin is shown in Figure 8.
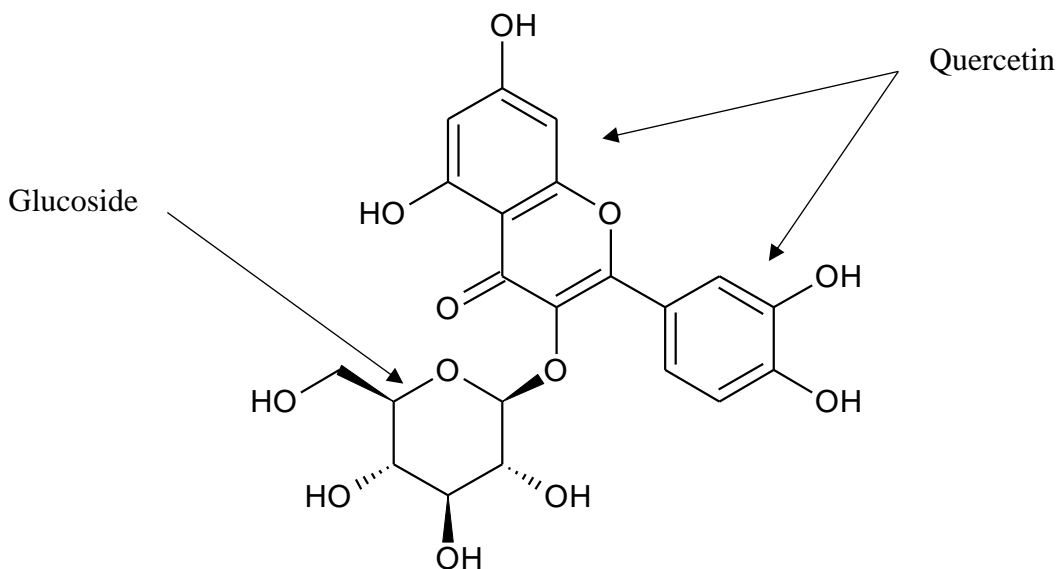
Figure 8. Isoquercetin (quercetin-3-O-beta-glucoside) chemical structure.

Capillary Electrophoresis

The use of electrophoresis as a separation technique was first introduced by Tiselius, who found that protein mixtures in a tube would separate based on two intrinsic properties of the proteins. When exposed to an electric field, the proteins would separate based on their charge and mobility in the solution[11]. This concept is often heard of with gel electrophoresis and can be used for the separation of DNA and proteins through a gel matrix. While this method of separation does work, it has several downsides which include: long separation times, low efficiency, and difficulty with sample detection and automation of the separation process. These separation disadvantages can be mitigated using capillaries with inner diameters of roughly 25-150 µm rather than gel slabs in the several centimeter range[11]. Increasing efficiency and lessening separation time is achieved using a higher voltage (kV

range) across the capillary. Any Joule heating produced from the high voltage separation in the capillary can be removed because the surface area to volume ratio is high[11]. The high voltage allows separation efficiencies of 10^5 theoretical plates or more. Additionally, the capillary electrophoresis (CE) process and sample analysis can be automated[11]. These attributes of CE and its wide range of areas of application make it very useful as a separation technique.

Two important CE components are an inlet reservoir that acts as an anode and an outlet reservoir that acts as a cathode. The sample is inserted into the capillary by pressure or electrokinetically, flows through the capillary, and is simultaneously separated. The sample can then be analyzed using various methods of detection such as UV-Vis spectroscopy or Laser Induced Fluorescence (LIF)[11]. The sample then exits through the outlet reservoir. The high voltage current that is passed through the buffer in the capillary is extremely important in inducing the process of separation. In typical separation techniques that use pressure as the driving force through a column or capillary, the flow of the sample is laminar and different areas of the flow are moving at different velocities[11]. In CE the flow is electroosmotic and the movement of the sample through the capillary is much more uniform, resulting in less zone broadening. This flow moves all species in the sample regardless of charge. The electrophoretic mobility of cations increases migration velocity, while that of anions decreases migration velocity. The small cations move in the shortest migration time towards the cathode followed by large cations, neutral species, large anions, and small anions[11]. The more positively charged species will also migrate faster and the more negatively charged species will move slower. The inside of the capillary consists of silanol groups which become deprotonated in the initial step of capillary rinsing with sodium hydroxide. The

groups then electrostatically interact with cations in the buffer. Capillary electrophoresis is not considered chromatography because the silanol groups do not interact with the sample, thus there is no stationary phase. The capillary electrophoresis setup can be seen in Figure 9.

When using CE a neutral marker may be employed to determine which peaks are the result of positively or negatively charged species. The neutral marker moves as a result of the electroosmotic flow and is not moving as a result of charge. When a neutral marker passes the detector, any species detected before it will be cations and any species detected after it will be anions. Additionally, if there is already an existing peak in the neutral marker peak area, then one may consider using micellar electrokinetic chromatography (MEKC) to successfully separate neutral species for analysis.
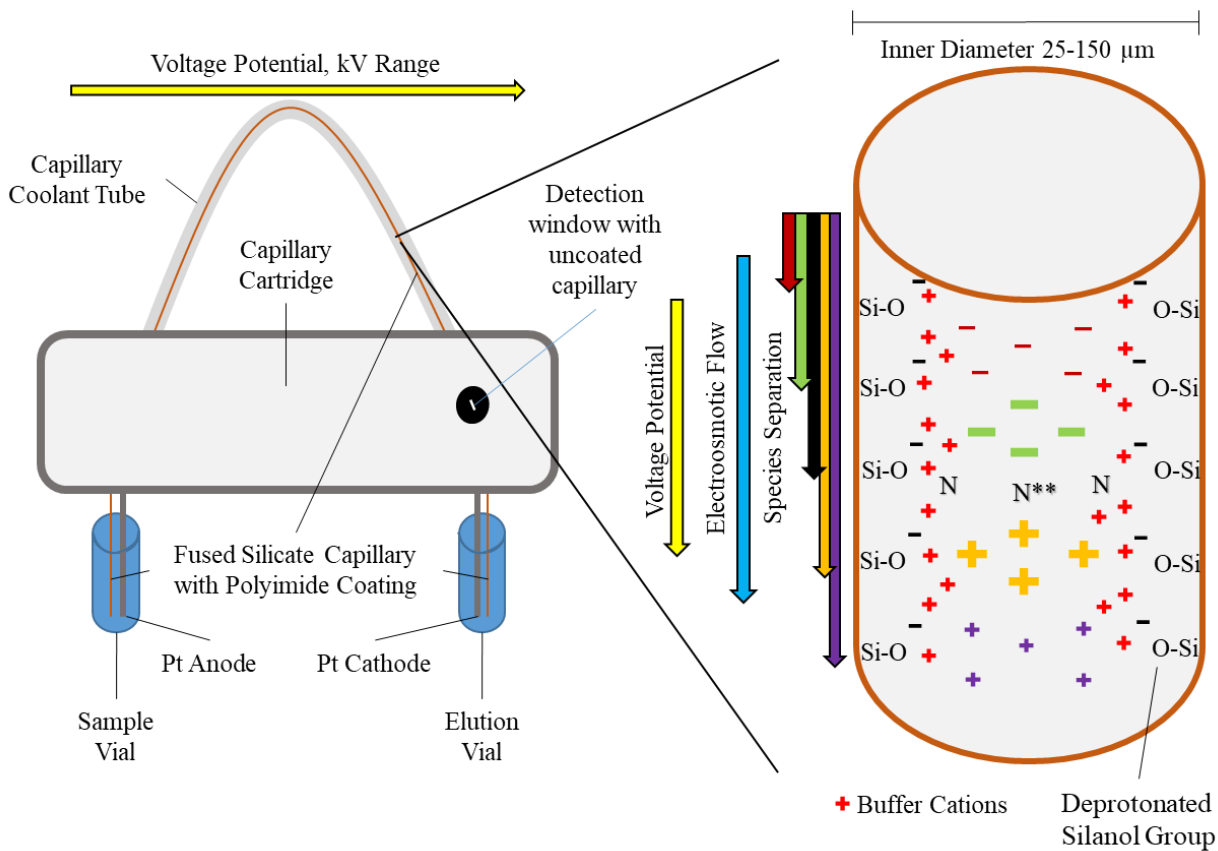
Figure 9. CE cartridge and functional components of the capillary.

Experimental Methods

<u>Plant Extraction</u>

       Over 2.0 g of *M. oleifera* leaf powder was ground in a spice blender to produce uniform particle size. Plant leaf particle size has been an important factor in changing quantities of certain extracted chemicals[12]. A microscopic image of a wet mount of ground leaf powder is shown in Figure 10. While particle size is beyond the scope of this project, these images may serve as a reference to particle sizes for future extractions. A resulting 1.9999 g of leaf powder was placed into a 100-mL round bottom flask with 50.00 mL of 200 proof ethanol. The mixture was allowed to reflux for 30 minutes and total extraction time was around 45 min. The resulting extract was vacuum filtered using a Whatman #1 filter to remove leaf debris. The filtrate was then placed into an Erlenmeyer flask designed for vacuum filtration. The extract was vacuum dried in a hot water bath by vacuum aspiration. In the Erlenmeyer flask 20.00 mL of 10 mM borate buffer was added. The borate buffer was made with sodium tetraborate at a 100 mM concentration and adjusted to pH 9.00 with 6 M HCl. The resulting buffer was diluted to 10 mM for use in the experiment. The residue from the extract was scraped loose from the flask walls into solution and the Erlenmeyer flask was vortexed for several minutes. The resulting mixture was filtered again with a Whatman #1 filter to remove most of the insoluble components and then decanted into a Falcon tube for storage at -20 °C. A pictorial representation of the extraction process is shown in Figure 11.
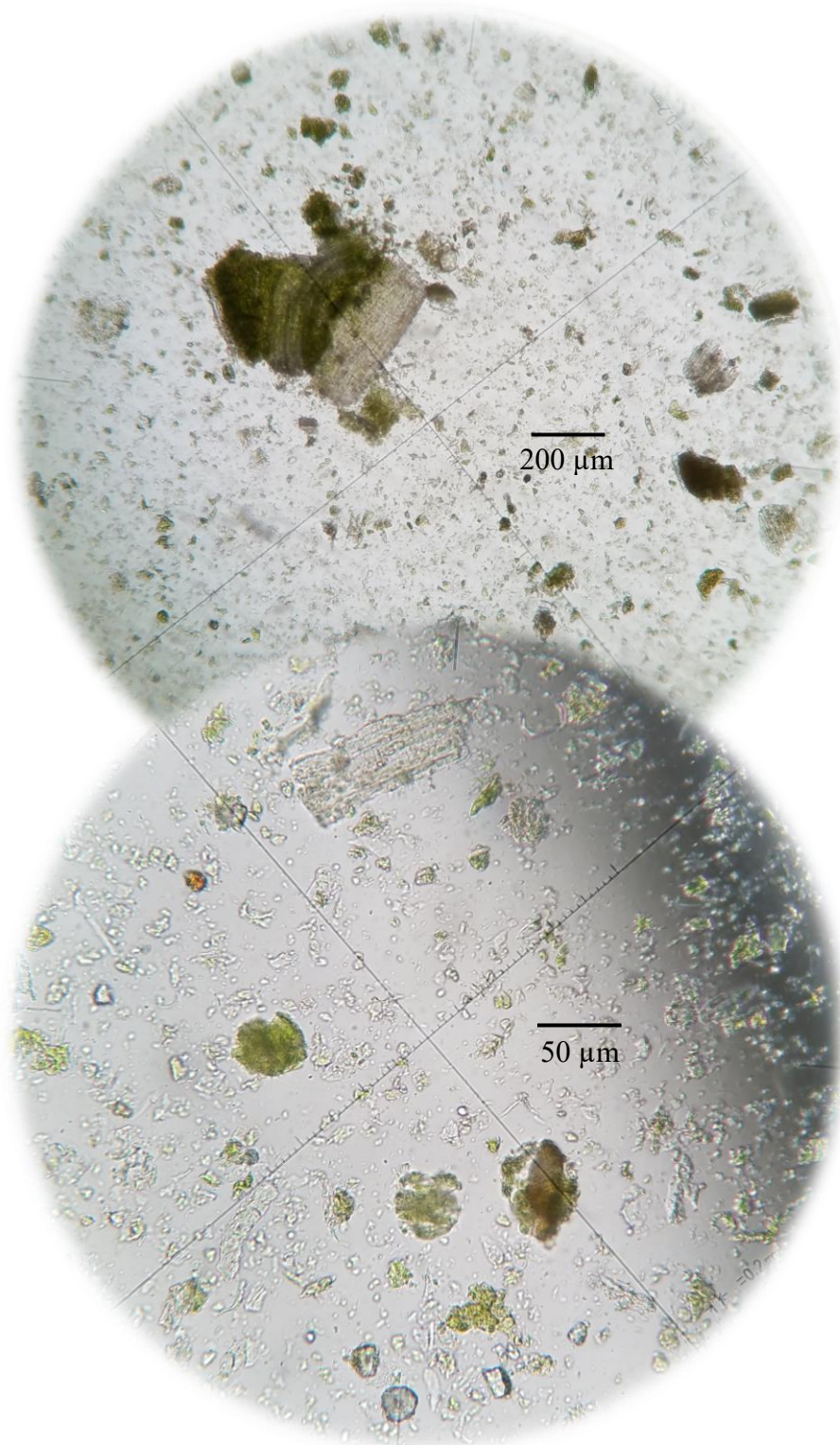
Figure 10. Microscopic images of a wet mount of *M. oleifera* leaf powder particles after grinding. Images were taken using a Leica DM EP polarizing light microscope with a calibrated ocular micrometer.

M. oliefera Plant Extraction Procedure

1. Dry leaf material was ground using a spice grinder

2. Extraction began with 25.0 ml of 200 proof ethanol per 1.0 g of leaf powder

3. Ethanol was allowed to reflux for 30 minutes

4. Extract was vacuum filtered with a Whatman # 1 filter and decanted into a vacuum filter flask

5. Extract was vacuum dried while in a hot water bath

6. 10.00 ml of 10 mM borate buffer were added to the dried extract per 1.0 g original leaf powder

7. The extract residue was scraped from the flask walls and the flask was vortexed

8. The extract was vacuum filtered again with a Whatman #1 filter and stored in a Falcon tube at -20°C

Extract Ready for Analysis

Ground leaf powder

Leftover leaf powder

Reflux setup

Dried extract

Vacuum drying apparatus

Dried extract with buffer

Vacuum filter apparatus

Aqueous insoluble components

Turbid final extract in buffer at desired concentration

Figure 11. Transcribed and pictorial representation of *M. oleifera* extraction procedure.

<u>Sample Analysis</u>

Samples used for analysis were collected from the frozen extract. The extract was allowed to thaw and was homogenized by vortexing. A sample of the extract was collected and filtered through a 0.22 µm syringe filter. The extract was then either placed quantitatively in quartz quvette and diltued for fluorescence and absorbance, or into a CE vial for standard addition and neutral marker analysis. All dilutions were made using 10 mM borate buffer at pH 9.00. Absorbance, fluorescence, and capillary electrophoresis data were collected in a Nanodrop spectrophotometer, Fluoromax-4 fluorometer, and a P/ACE MDQ Beckman Coulter CE instrument respectively. The capillary inner diameter for CE was 50 µm and was 59.8 cm in length. Before sample separation the capillary was rinsed with 1.0 M NaOH followed by deionized water, and then 10 mM borate buffer at pH 9.0. Each rinse was performed for three minutes at 40 psi. Sample pressure injection time was 15 sec at 0.5 psi and sample separation occured at 20kV.

Absorbance

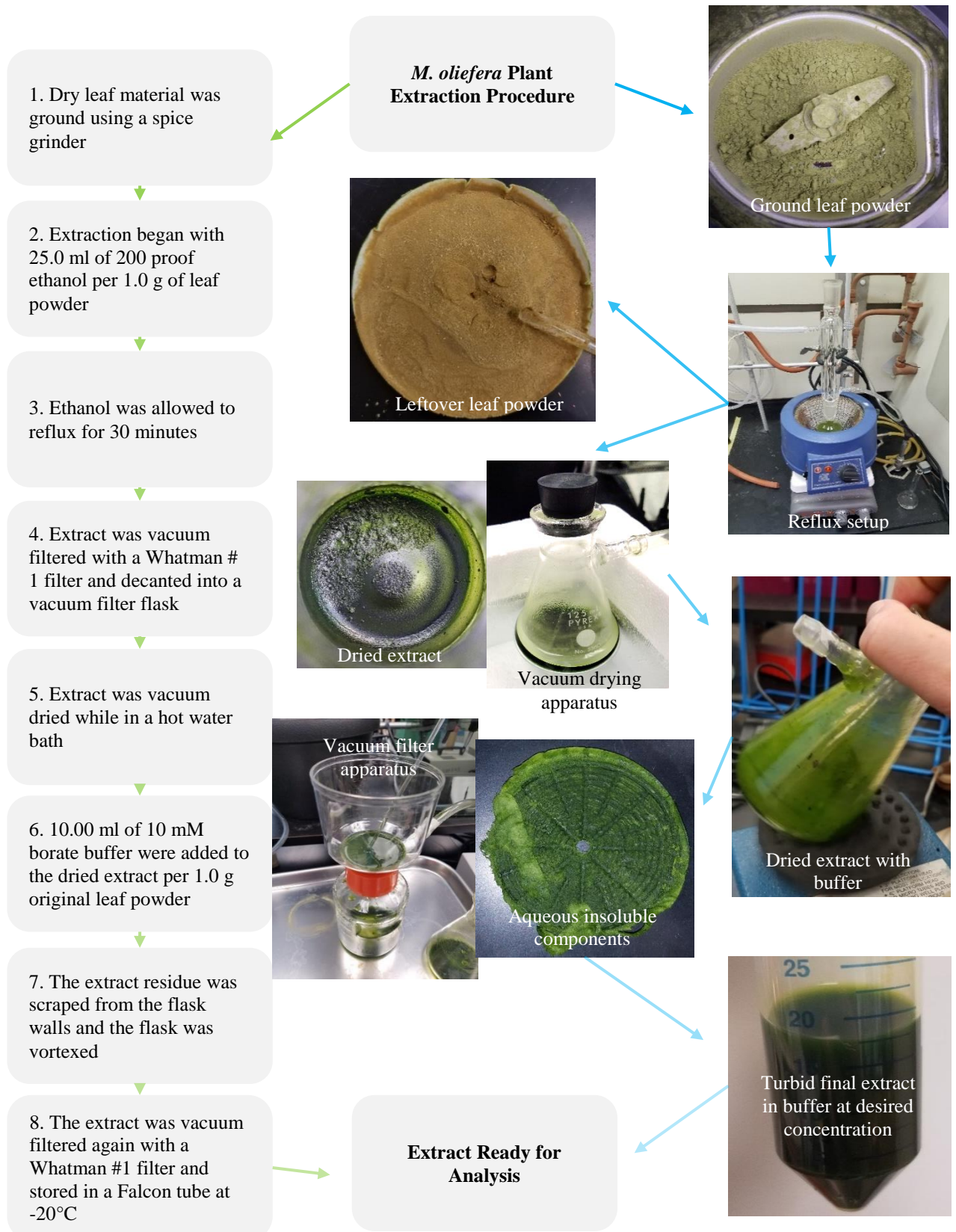Absorbance data was collected with a spectrophotometer and a quartz cuvette. The spectrophotometer was blanked before each absorbance with buffer. For extract analysis a 1:99 dilution of extract to buffer was performed. For isoquercetin analysis, a 1:24 dilution of stock solution to buffer was performed.

Fluorescence

Fluorescence emission data was collected with a fluorimeter and samples were placed in a quartz cuvette. For extract analysis a 1:99 dilution of extract to buffer was performed and excitation and emission slit widths were decreased to 3 nm. For isoquercetin analysis, a 1:24

dilution was performed and excitation and emission slit widths were kept at 5 nm. Both

samples were excited at 355 nm.

Standard Addition

The standard addition method was used with a chemical standard of isoquercetin ≥

90% by HPLC (CAS # 48-35-9) from Sigma Aldrich Lot # BCBW0300. The stock solution

was made with 0.0082 g of isoquercetin standard in 25.00 mL of borate buffer. Solutions

used in the standard addition and their respective details are tabulated in Table 1. Absorbance

detection for the standard addition was at 340 nm and peak area was integrated. Separate

rinsing and buffer vials were used for each spiked sample to avoid changes in the separation.

Solution Type	Isoquercetin Concentration from Standard µM	Extract Added µL	Buffer Added µL	Stock Solution Added µL	Total Volume µL
Isoquercetin Stock Solution	706	N/A	N/A	N/A	N/A
Spiked sample #1	0	500	1000	0	1500
Spiked sample #2	471	500	0	1000	1500
Spiked sample #3	333	500	292	708	1500
Spiked sample #4	235	500	500	500	1500
Spiked sample #5	133	500	717	283	1500
Spiked sample #6	67	500	858	142	1500

Table 1. Solutions used in the standard addition and their respective details.

The uncertainty for the concentration of isoquercetin at the x-axis was calculated

using the following equation

$$u_x = \frac{s_y}{|m|} \sqrt{\frac{1}{n} + \frac{\bar{y}^2}{m^2 \sum (x_i - \bar{x})}}$$

where s_y is the standard deviation of y, m is the slope of the trend line, n is the number of

data points collected, $\bar{y}$ is the mean of the peak area, x_i is the concentration isoquercetin in

the spiked samples, and $\bar{x}$ is the mean of the isoquercetin concentrations of the spiked

samples. The LINEST function in Excel was used to calculate s_y and m, which are gathered

from a linear trend line. The absolute value of the trend line x-intercept corresponds to the

concentration of the diluted unspiked sample. This value was multiplied by three to account

for the dilution of spiked sample # 1 in Table 1.

Neutral Marker

Mesityl oxide (CAS # 141-79-7) from SPEXOrganics® Lot # TS170412007 was

used as a neutral marker and was of 90% purity. A sample of the diluted extract with 150 µL

of mesityl oxide, a sample of diltued extract, and a sample of 100 µL of diluted mesityl oxide

was used to determine the mesityl oxide location on the electropherogam. Absorbance

detection on the CE instrument was at 254 nm.

Hydroponic and Growth Chamber Model

The hydroponic growth chamber was designed to minimize the effects of several

variables such as lighting, water fluctuations, and nutrient availability. The plants were

exposed to two different types of compact fluorescent lights (CFL). The first was designed to

mimic daylight spectrums and has a spectral output from the 200-700 nm range. The second

bulb had the same spectrum output range, but with different intensities in certain areas,

especially in the UV range. The spectrums for these two bulbs is shown in Figure 12. Part A

depicts the UV dominant bulb which is designed for UVA and UVB output and part B

depicts the PAR dominant bulb with a slight amount of UVA output. Bulb A was set to turn on for two hours a day during the time that bulb B was set to turn on for 12 hours a day.
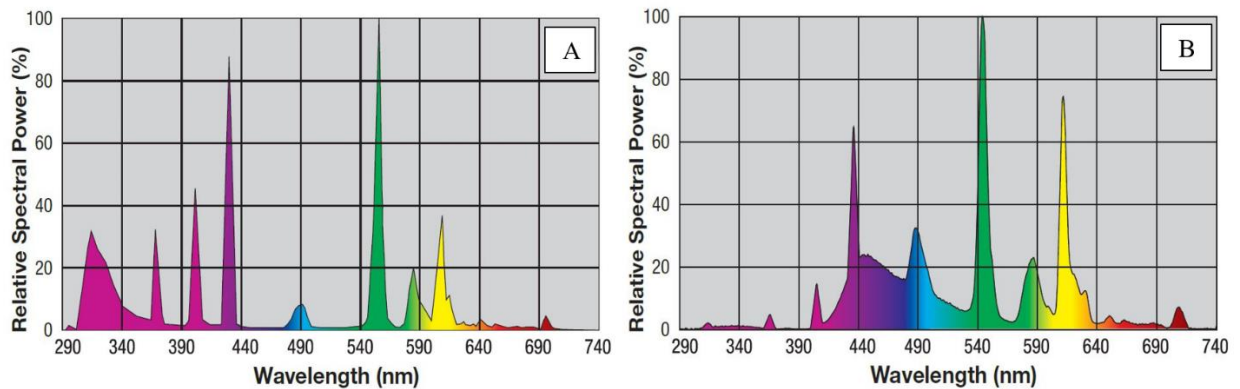

Figure 12. Fluorescent light bulb spectrum for two separate grow bulbs A and B[13].

The growth chamber setup is depicted in Figure 13. The rotation of the grow raft allowed for more even lighting between the two types of CFL bulbs in the growth chamber. This was achieved using a water pump in the bottom of the bucket that was angled in such a manner to induce a vortex. Additionally, the pump induced a Venturi powered suction of air and aerated the water. The Styrofoam grow raft (originally a holder for test tubes) floated on top of the water and contained *M. oleifera* seeds. Water used in this setup was distilled in order to reduce the effects of nutrient availability. The setup also included a heating pad designed for germinating seeds in seed trays. The pad was wrapped around the bucket and warmed the water to optimize plant growth. The UVA and UVB intensity of the bulbs in the growth chamber was measured using a Vernier UVA and UVB sensor. A graphical display of this data is shown in Figure 13. The optimal growing height range for the plants would be in the part of the curve with the least amount of change in intensity as height increases. This area is the closest to the grow raft and is highlighted in purple.
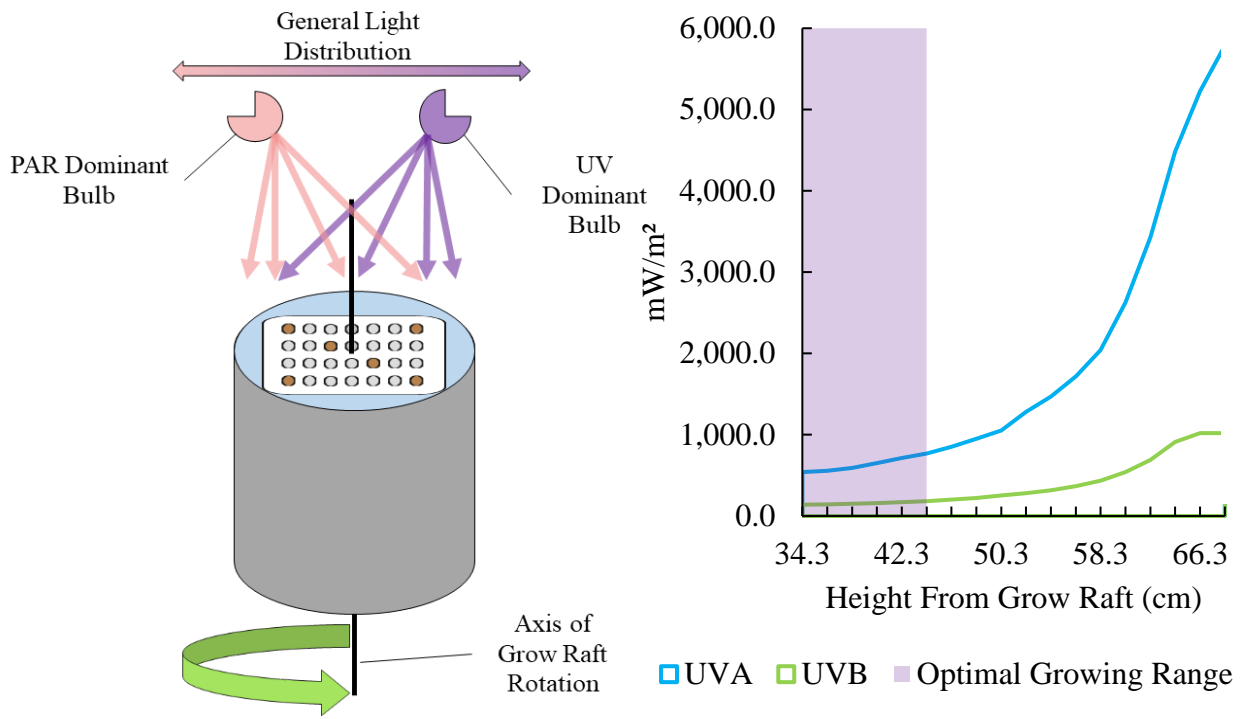
Figure 13. Graphical representation of hydroponic setup and UVA and UVB intensity vs. height from the grow raft.

Results

<u>Absorbance</u>

Extract absorbance was the most prominent in the 300-400 nm range (Figure 14). A small peak around 670 nm was also in the extract absorbance curve. Isoquercetin absorbance was the most prominent between 300-400 nm. Shoulders overlapped on the absorbance curves at around 330 nm.
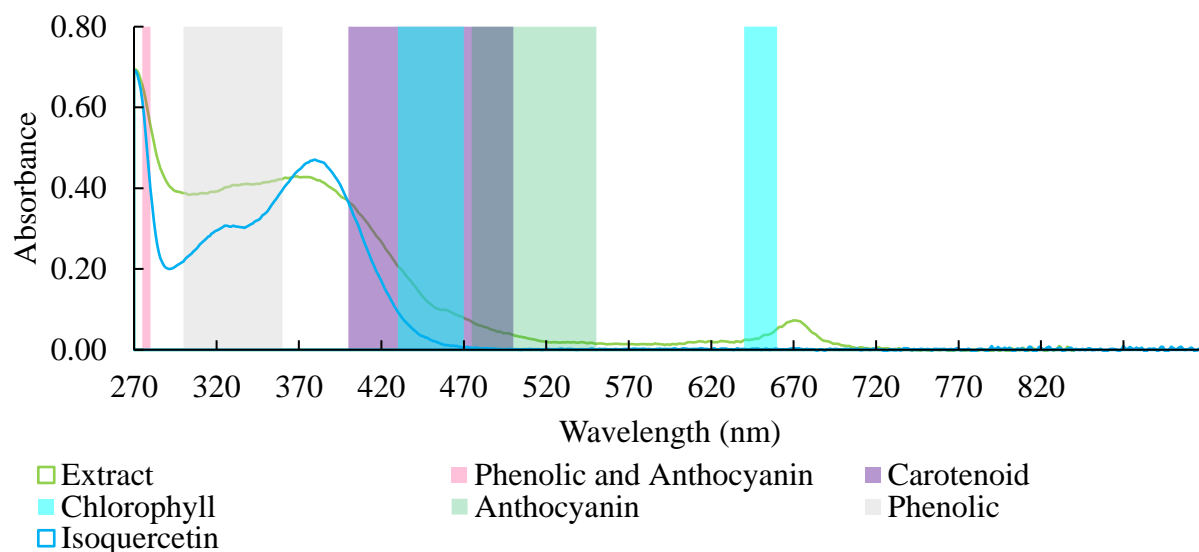
Figure 14. Absorbance curves for extract and isoquercetin samples. Phytochemical class absorbance ranges are overlapped on the graph[6,7].

The fluorescence emission curve for the extract was the most prominent in the 400-600 range (Figure 15). A small peak on the extract curve appeared at 675 nm. The curve for isoquercetin had a small peak at 403 nm and a minor amount of emission from 415-665 nm. A shoulder on the extract curve overlapped with the small peak from isoquercetin at 403 nm.
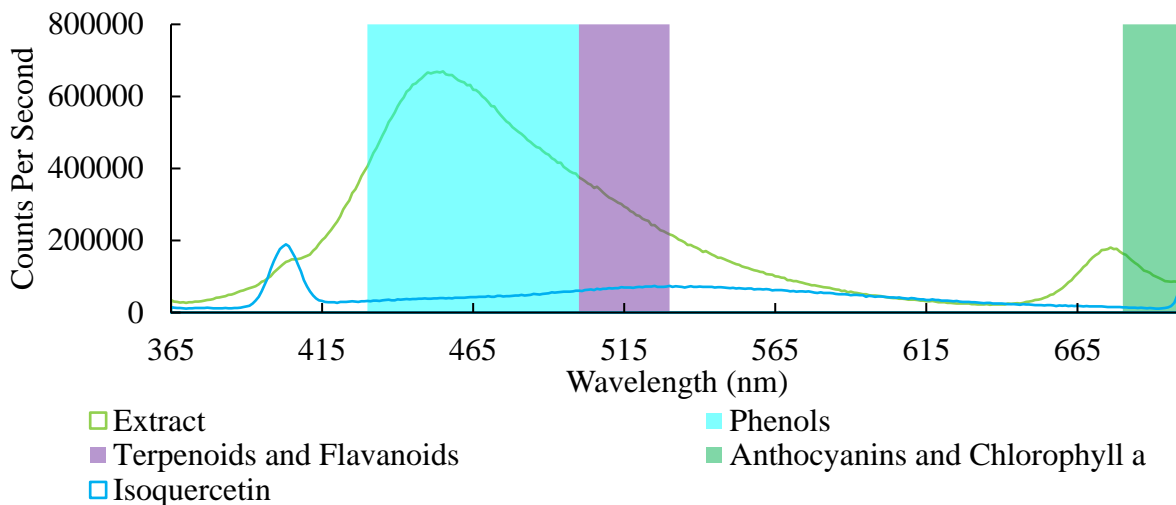
Figure 15. Fluorescence emission curves for extract and isoquercetin samples excited at 355 nm. Phytochemical class fluorescence ranges are overlapped on the graph[14].

Capillary Electrophoresis

Neutral Marker

A mesityl oxide peak appeared at the very beginning of peaks in the electropherogram around 3.9 minutes (Figure 16). There was little fluctuation in migration time between the mesityl oxide and the mesityl oxide with extract.
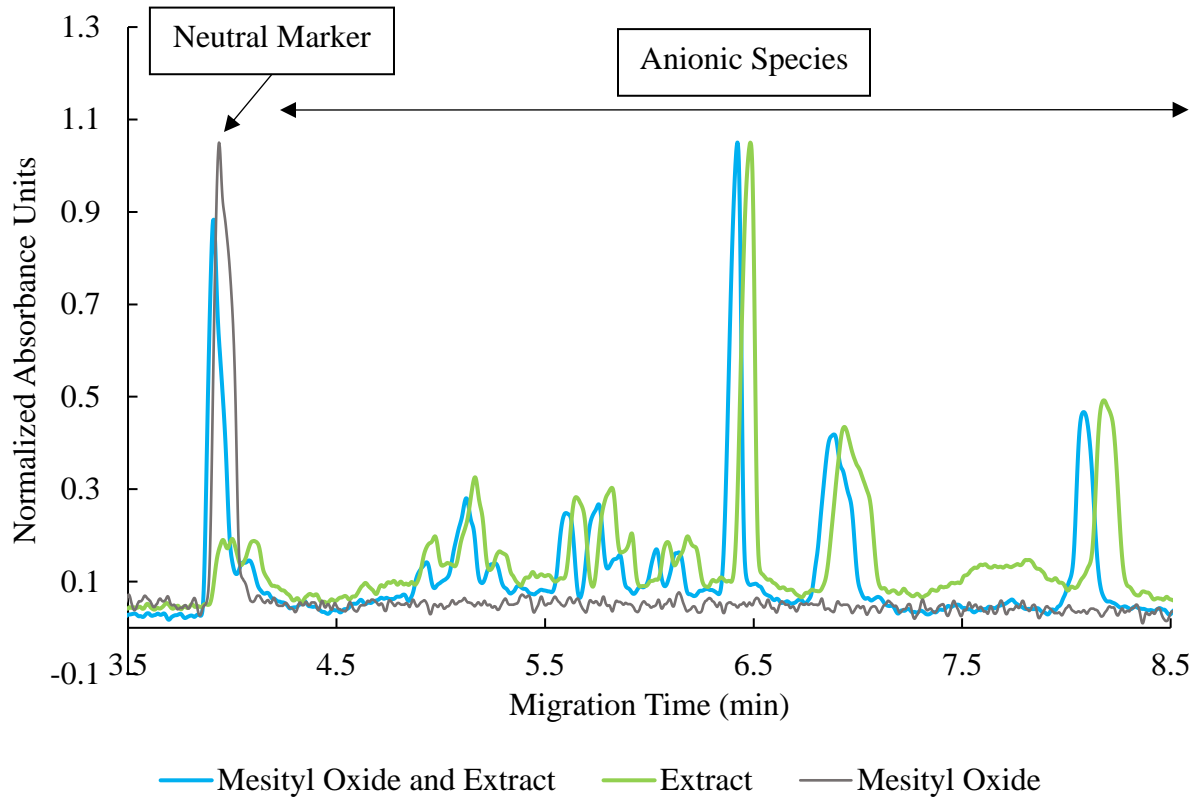
Figure 16. Neutral marker mesityl oxide with extract, extract, and mesityl oxide on an electropherogram. Absorbance has been normalized and 0.05 was added to offset data for visualization. All anionic species are present after the neutral marker.

Standard Addition

The spiked samples showed an increase in the absorbance of a large peak around 6.5 minutes migration time as shown in Figure 17. The migration time for all the peaks were slightly lengthened with the spiked sample. This representative graph contains electropherogram data for a sample containing just extract and buffer and a sample of extract with a spike which corresponds to spiked sample # 4 in Table 1.

Figure 17. Electropherogram showing the peak area increase following a spike of isoquercetin.

The standard addition graph is shown in Figure 18. The trend line produced an R^2 of 0.9921 and points corresponding to spiked samples # 2 and 6 were the most imprecise.
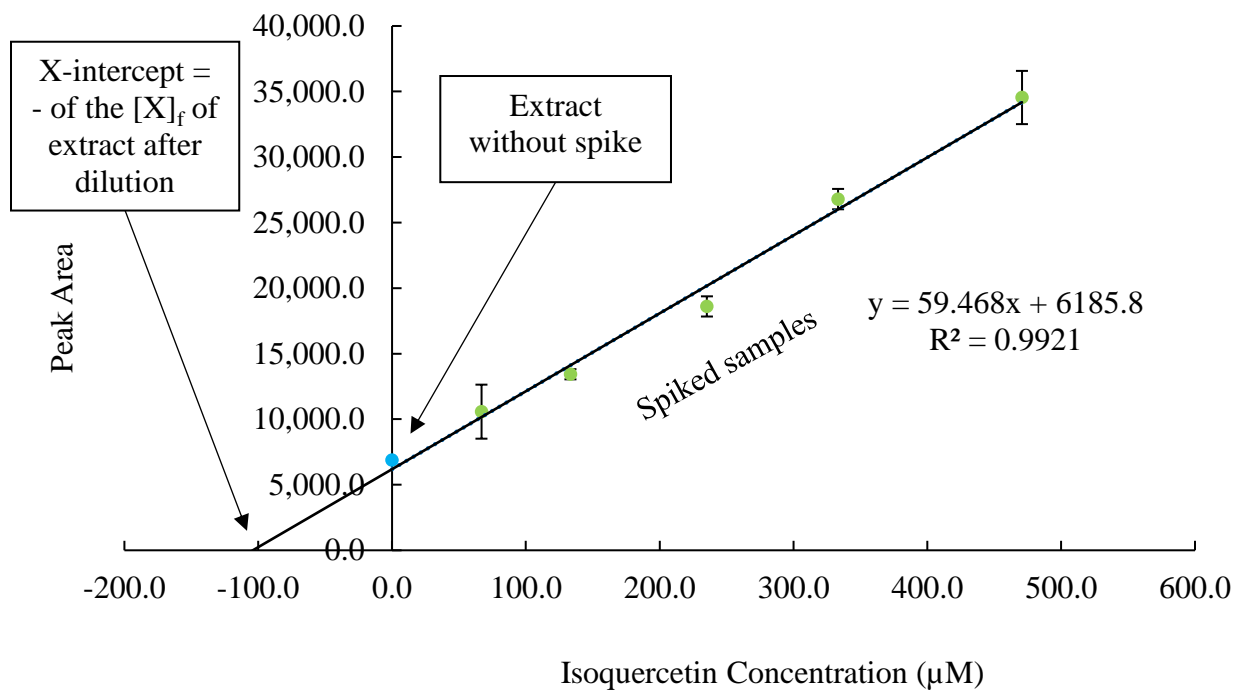
Figure 18. Graph of standard addition of isoquercetin in *M. oleifera* extract.

The calculated x-intercept value was 104 ± 14 µM meaning that the final calculated concentration of isoquercetin in the *M. oleifera* extract was 312 ± 42 µM.
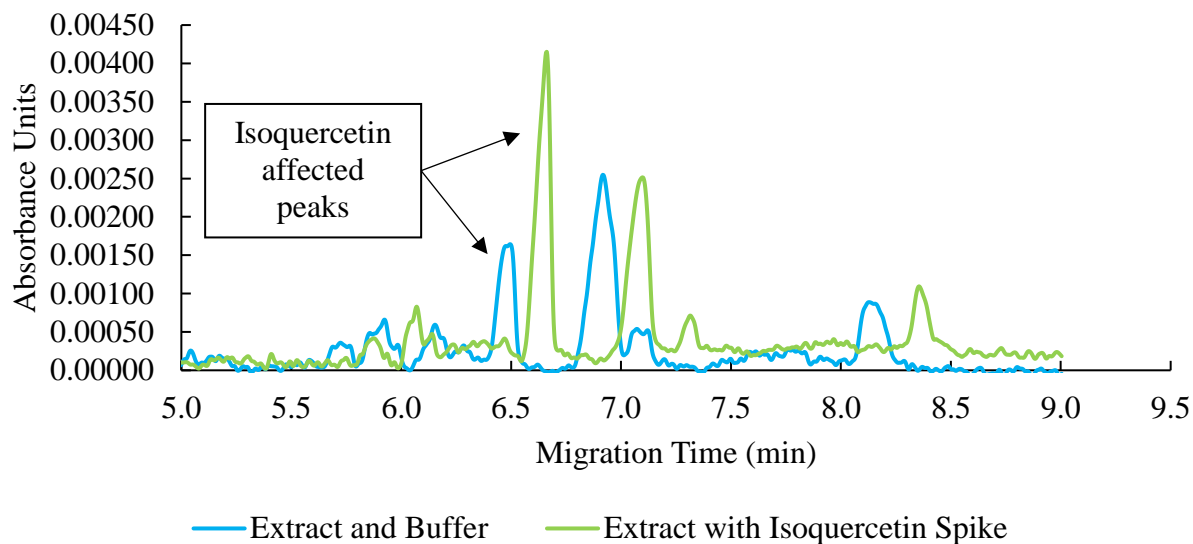
Growth Chamber Setup

Viable leaf material for extracts was available in roughly 18 days of growth using the bucket setup prototype as shown in Figure 19. This growth was supported by minute quantities of light from a window. Plant growth appeared normal in morphology.

Figure 19. Growth of *M. oleifera* over 18 days using the bucket prototype.

The process was repeated in the bucket setup using the growing chamber and UV supplemented lighting. The result of this after 18 days is depicted in Figure 20. Most of the seedlings grew in the growth chamber, but not as expected. Viable leaf material was present as shown in Figure 18. Root growth was not optimal (Figure 21) and not the same as root growth in Figure 17. Additionally, the leaves depicted in Figure 19 were dry and brittle despite the bottom of the plant being wet.
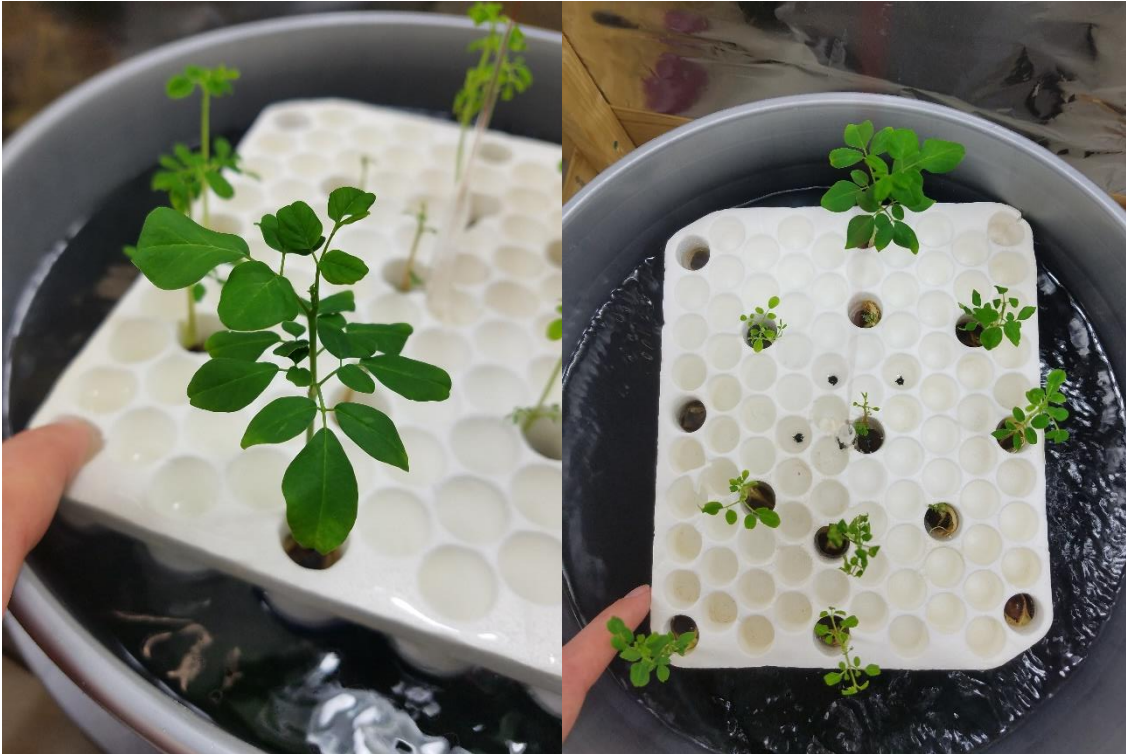
Figure 20. Plant growth after 18 days using the growth chamber.

Figure 21. Root growth problems with an unidentified cause.

Pink pigmentation was produced along the stem of some of the seedlings and is shown in Figure 22. A 200x microscopic image of stem tissue with the pigmentation is shown along with a seedling showing pigmentation.
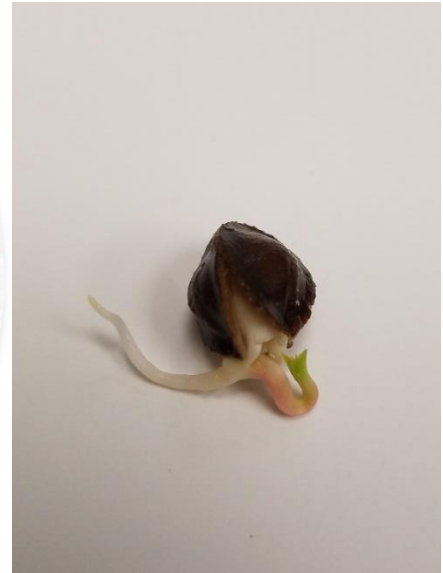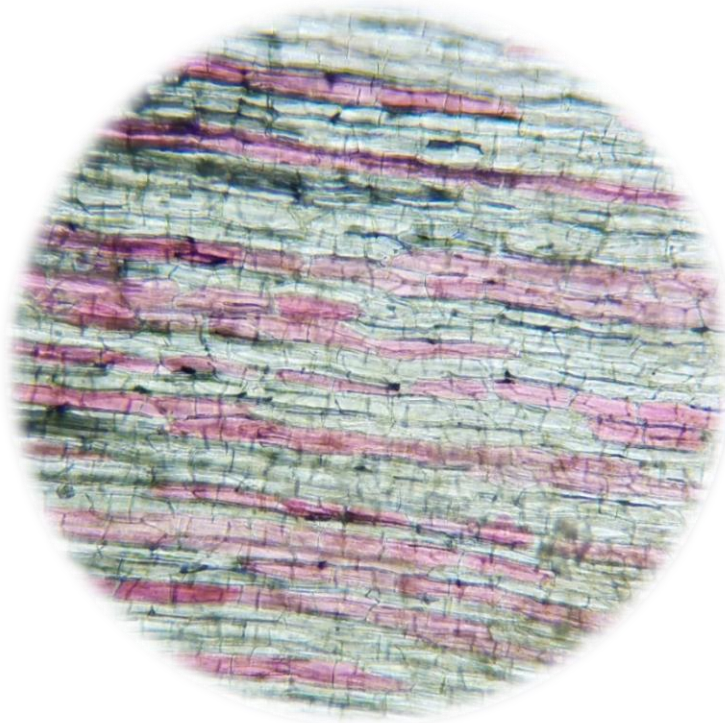
Figure 22. Pink pigmentation in *M. oleifera* stem tissue 200x microscopic image on the left and seedling pigmentation on the right. The microscopic image was taken with an Omax binocular compound microscope.

Discussion

Moringa oleifera Extract

Extraction

The effectiveness of a plant extraction has been correlated with the removal of chlorophyll from the plant material. It is also recommended to use 70% ethanol when doing a plant extraction[7]. The residual plant material from the first extract filtration was brown in color and contained no visible chlorophyll, likely indicating a successful extraction (Figure 11). A solvent consisting of 70% ethanol may work better than ~100% ethanol for extraction, but it was not employed in this experiment due to its longer extract drying time. Further work on changing the extract parameters may result in a better extraction for future experiments.

Absorbance

The extract absorbance in Figure 14 had absorbance in the phenolic and anthocyanin ranges. This was likely the result of aromatic rings on many of the phytochemicals. There was also absorbance in the carotenoid, chlorophyll, and anthocyanin ranges. There was some absorbance near the chlorophyll range at 650 nm, but the majority of the small peak was outside this range. The peak was likely from chlorophyll as the extract was green and was produced from green plant material. The red shift away from the region may have been a result of the extract being more of a complex matrix of phytochemicals or the effects of the buffer. The isoquercetin had absorbance in the same general area as the extract, but did not show the same peak around 670 nm. This made the absorbance of the extract less revealing as the isoquercetin was under the same general area. There was however a small shoulder on the extract absorbance around 325 nm that was directly over a similar shoulder on the

27

isoquercetin absorbance curve. The shoulder on the extract may have been indicative of the presence of isoquercetin.

Fluorescence

The fluorescence emission curve for the extract (Figure 15) was more prominently in the phenol range, but also included terpenoids and flavanoid ranges. There was also another peak at 675 nm which was likely chlorophyll, but was blue shifted from the chlorophyll range. The isoquercetin curve showed slight emission at 403 nm which was outside any of the ranges for phenols and flavanoids. There was, however, minor and broad emission in the flavanoid region. Similarly to the absorbance findings, there was overlap in the curves at 403 nm. The small shoulder on the extract curve was over the small peak from isoquercetin. This was another indication that isoquercetin was likely in the extract. The large amount of fluorescence in the phenol range could mean that there are several other phenolic phytochemicals in the extract that may be of interest.

Neutral Marker

The mesityl oxide peak started at roughly 3.9 minutes of migration time (Figure 16). The peak present in the mesityl oxide and extract was clearly not visible in the extract alone. The mesityl oxide also appeared at the same migration time when mixed with buffer alone. This further reinforced the likelihood that the peak was from mesityl oxide. Based on this information, it can be stated that all of the remaining peaks after the mesityl oxide were the result of anionic species and there were no cationic species that absorbed at 254 nm. This was because anionic species are the last to elute from the capillary since they oppose the cathode but still move with the EOF. There were also no peaks present before the mesityl oxide peak. The placement of the mesityl oxide also meant that MEKC was not necessary for

standard addition analysis because the peak analyzed for standard addition was not composed of neutral species. If it had been, additional separation with MEKC would have been necessary before standard addition analysis.

Standard Addition

The standard addition of isoquercetin was visible on the electropherogram (Figure 17). The peak around 6.5 minutes in the extract with buffer increased by roughly two fold in absorbance units with the extract and isoquercetin spike. The peak also increased while all the other peaks in the electropherogram were visibly similar in absorbance units. There was a shift in migration time between the two samples, but migration time was visibly proportional across the electropherogram indicating that separation was the same.

The standard addition data gave an R^2 value of 0.9921 (Figure 18). This was not an ideal correlation for quantitation, but it does signify that the relationship between concentration and peak area for isoquercetin is linear. Spiked samples # 2 and 6 were the most imprecise and could have been improved in precision with more trials. Additional trials also would have allowed for better statistical analysis to remove an outlier. The absolute value of the x-intercept was calculated to be 104 ± 14 µM. When factoring in the dilution of the extract, the resulting concentration of the original extract was 312 ± 42 µM. This was a large range of uncertainty and indicated that a repeat experiment would be necessary before conclusive statements can be made about the concentration of isoquercetin in the extract. Changing some of the parameters on the CE instrument may result in more reliable data. Such parameters may include separation voltage, pressure injection time, and increasing the concentration of the sample. One important note to consider is that the capillary used in this experiment had a path length of 50 µm where some absorbance measurements are taken with

10,000 μm path lengths. An increase in the extract concentration may make noise more negligible on the electropherogram and result in more precise data. An additional possibility to improve data would be through the use of LIF, which could improve detection at lower extract concentrations over the 50 μm path length. However, one would have to be sure that isoquercetin was excitable at the set laser wavelength.

Hydroponic and Growth Chamber Model

The prototype for the growth chamber model grew *M. oleifera* plants well within an 18 day window (Figure 19). The morphology of the plants appeared consistent with that of healthy growing plants. The same was not true for the plants grown in the finished model. One plant shown in Figure 20 had what appeared to be normal morphology in terms of leaves, but barely had any root structure. Many of the other plants had smaller leaves indicating a slower development, or a change from normal morphology. A total of 14 plants were placed in the grow raft; five of them never developed leaves, eight of them developed minimal leaves, and one developed optimal leaf material. This would heavily impact the continuation of the experiment because leaf material is needed to make extract for analysis. Additionally, if root growth is inhibited (Figure 21) by an unknown cause, it may adversely affect the results produced by the analysis of the leaf extract. Ideally, the plants would show healthy characteristics before making an extract. One possible cause of the root growth problem could be the use of distilled water. The plants grown in the prototype grew in hard well water. Another possible problem could be the UVB and UVA lighting. The UVA exposure in the growing range of the plants was about four times as intense as the UVB exposure. One reference states that under normal environmental conditions UVA intensity is 10 to 100 times that of UVB[5]. Plants also seem to respond differently to UV stimuli, so

further testing with and without a UV stimulus would be useful.

Some, but not all of the plants grown in the model displayed a pink pigmentation on the stem (Figure 22). This was likely anthocyanin pigmentation in response to the UV stimulus as anthocyanins can be photo-protective. The pigmentation was also not visible on the plants grown with the prototype which had no UV lighting.

One important consideration in the bulb selection for the model is the low intensity output in the red region of the visible spectrum (Figure 12). Both chlorophyll a and b have absorption in the orange to red region of the visible spectrum[7]. This may adversely affect the usefulness of this model, but the cost and waste heat hazards from running better spectrum lighting (such as metal halide) are largely reduced using this form of lighting. More natural lighting spectrums with Light Emitting Diode (LED) bulbs may produce healthier plants, but they do not commonly come with UV capabilities.

Conclusion

This project focused on two goals. The first was to develop an extraction procedure, and analyze the extract for isoquercetin and other phytochemicals using absorbance, fluorescence, and capillary electrophoresis. The second was to develop a growth chamber model with UV supplemented conditions and use it to grow *M. oleifera* in the hopes of stimulating more beneficial phytochemicals. These plants would then be analyzed using the same methods of absorbance, fluorescence, and CE. The first goal was completed and absorbance and fluorescence data presumptively indicate the presence of isoquercetin the extract. The neutral marker confirmed that MEKC was not necessary for the standard addition of isoquercetin. The standard addition trend line had an R^2 of 0.9921 and the extract isoquercetin concentration was calculated to be 312 ± 42 µM. The uncertainty of this concentration likely means that a repeat experiment would be necessary before making conclusive statements about the isoquercetin concentration. This does, however, indicate that there is a linear relationship of concentration to peak area for isoquercetin. The second goal was not completed as the *M. oleifera* plants had abnormal morphology and did not produce a large quantity of leaves when grown in the final model. They did, however, show some pink pigmentation which is likely the result of anthocyanins. Other less obvious photo-protective phytochemicals may be present as a result of the UV supplementation.

Future Work

Moringa oleifera Extract Analysis

        The extraction procedure of *M. oleifera* could be further optimized to reduce extraction time and resource usage without reducing phytochemical quantities. This may include steps such as reducing reflux time and using less ethanol for extraction. An additional standard addition with more trials could result in more precise and accurate data. This method could also be employed with other phytochemical standards known to be in *M. oleifera.* Additional work such as tandem mass spectrometry (MS/MS) could serve as a confirmation of the peak identity used for the standard addition data. MS/MS is similar to mass spectrometry (MS), but it consists of two or more mass spectrometers. A large difference in MS/MS compared to MS is the separation of the ions generated from the first ionization source and their further use in another MS. The parent ions of a certain mass to charge ratio (m/z) undergo a reaction to create further dissociation[15]. These dissociated parent ions become product ions that then travel into the second MS to be further separated. The attributes of MS/MS are particularly useful for the analysis of complex mixtures because of the aforementioned additional separation step[15].

Hydroponic and Growth Chamber Model

        Before the growth chamber model plants can be used in further research, the problem of root growth needs to be addressed. Since the source of the problem is unknown, it may take time to correct the problem. Once plants with normal hydroponic morphology are available under the growth chamber conditions, the plants can be analyzed using the steps previously mentioned with extract analysis. Then these can be compared to a control without

UV lighting. This should aid in determining if UV exposure is useful for stimulating

phytochemicals like isoquercetin.

References

(1)   Csurhes, S.; Navie, S. *Horseradish tree*; 2016.

(2)   Leone, A.; Spada, A.; Battezzati, A.; Schiraldi, A.; Aristil, J.; Bertoli, S. *Int. J. Mol. Sci.* **2015**, *16*, 12791–12835.

(3)   Stohs, S. J.; Hartman, M. J. *Phyther. Res.* **2015**, *29*, 796–804.

(4)   Remote Sensing: Absorption Bands and Remote Sensing https://earthobservatory.nasa.gov/Features/RemoteSensing/remote_04.php.

(5)   Verdaguer, D.; Jansen, M. A. K.; Llorens, L.; Morales, L. O.; Neugart, S. *Plant Sci.* **2017**, *255*, 72–81.

(6)   Solovchenko, a. E.; Merzlyak, M. N. *Russ. J. Plant Physiol.* **2008**, *55*, 719–737.

(7)   Harborne, J. B. *Chapman Hall* **1998**, 58.

(8)   Saleem, R. Studies in the Chemical Constituent of Moringa oleifera Lam., and Preparation of Potential Biologically Significant Derivatives of 8-hydroxyquinoline, University of Karachi, 1995.

(9)   Vongsak, B.; Sithisarn, P.; Gritsanapan, W. *Evidence-based Complement. Altern. Med.* **2013**, *2013*.

(10)   Orfali, G. di C.; Duarte, A. C.; Bonadio, V.; Martinez, N. P.; de Araújo, M. E. M. B.; Priviero, F. B. M.; Carvalho, P. O.; Priolli, D. G. *World J. Clin. Oncol.* **2016**, *7*, 189.

(11)   Lauer, H.; Rozing, G. *High Performance Capillary Electrophoresis - A Primer*; 2014.

(12)   Makanjuola, S. A. *Food Sci. Nutr.* **2017**, *5*, 1179–1185.

(13) *Reptile Lighting Guide*; Rolf C. Hagen: Mansfield.

(14) Solovchenko, A. *Photoprotection Plants Opt. Screening-Based Mech.* **2010**, *14*, 67–88.

(15) Glish, G. L.; Vachet, R. W. *Nat. Rev. Drug Discov.* **2003**, *2*, 140–150.